

Three-dimensional mechanical properties analysis and fatigue life prediction of G105 drill pipe

Kuan Zhao^{1,a}, Bangwen Wang^{1,b,*}, Jinping Li^{2,c,*}, Lamei Peng^{3,d}

¹School of Mechanical Engineering, Xi'an University of Science and Technology, Xi'an, 710054, China

²Engineering Research Center of Expressway Construction & Maintenance Equipment and Technology of MOE, Chang'an University, Xi'an, 710054, China

³Shaanxi Taihe Intelligent Drilling Company Limited, Xi'an, 710086, China

^axinkuan1022@xust.edu.cn, ^b21205224073@stu.xust.edu.cn, ^cljip@chd.edu.cn, ^dalison-plm@163.com

*Corresponding author

Abstract: G105 drill pipe has been widely used in drilling construction, such as mine exploration, water exploration, and gas extraction. However, the service life of the drill pipe is lower than its design life. The drill pipe is the most vulnerable component within the overall structure of the drilling tool due to its exposure to cyclic axial tension, torsion, and bending forces. Taking the G105 drill pipe as the research object, the mechanical property parameters and fatigue S-N curve of drill pipe material were tested by tensile test and tension-torsion multi-axis fatigue test. The geometric expression of the cross-section profile perpendicular to the drill pipe is derived, and a parametric three-dimensional finite element modeling method for the drill pipe is proposed. According to the relationship between the element and the node, a parametric three-dimensional hexahedral mesh modeling program for the drill pipe is developed. In conclusion, an examination is conducted on the mechanical characteristics of the drill pipe when subjected to various loads, including make-up torque, compression-torsion, and compression-bending-torsion. Additionally, a prediction is made regarding the fatigue life of the drill pipe under these multi-axial conditions. The results show that the maximum stress of the drill pipe under the combined load appears on the inner and outer surfaces of the drill pipe, and is most significant at the intersection of the transition section and the pipe body under the influence of stress concentration. The fatigue life of the pipe body is positively correlated with the wall thickness, and the minimum value of the multi-axial fatigue life of the drill pipe occurs in the vicinity of the interface between the transition section and the pipe body, so in order to improve the fatigue life of the drill pipe, it is preferred to give priority to the optimization of the structure or the surface reinforcement treatment in this place.

Keywords: Mechanical property; Parametric modelling; Borehole curvature; Fatigue life

1. Introduction

As an important means of "entering the earth", drilling is known as the "telescope extending into the earth". Due to its lightweight, disintegration, simple operation, and reliable use, drill pipe is the main component in the construction of geological exploration, oil and gas exploitation, mine water drainage, and gas drainage [1,2]. However, due to the cyclic action of composite loads, such as axial stress, torsion, and bending moment on the drill pipe during the drilling process, a large number of premature fracture accidents of the drill pipe have occurred in both domestic and foreign drilling constructions, resulting in huge economic losses [3,4]. Statistically, fatigue and brittle fracture account for the largest proportion of failure types, reaching more than 80% [5]. Therefore, it holds immense importance to investigate the mechanical properties of drill pipe materials under various working conditions and achieve fatigue life prediction in order to enhance the design methodology and life of drill pipe.

To enhance the operational efficiency of drill pipe and mitigate the occurrence of drill pipe failures, measures need to be implemented. Domestic and foreign scholars have carried out in-depth research on the mechanical properties and fatigue failure behavior of drill pipes [6-9]. The main research methods are the analytical method [10,11], the experimental method [12,13], and the finite unit method [14,15]. LI et al. [16] systematically analyzed the drill pipe from two aspects of material quality and stress, which mainly included testing and inspection of the morphology, chemical composition, mechanical properties, and metallographic and microfracture of the drill pipe material. GUO et al. [17] analyzed the fatigue failure behaviour of the drill pipe joint under extreme conditions. They found that the fatigue life of the drill

pipe can be prolonged by reasonably adjusting the rotation speed and drilling pressure. Zhu et al. [18,19] designed a high torsional double shoulder drill pipe joint, calculated the bearing capacity and fatigue performance of the joint, and obtained that the borehole curvature had a significant effect on the stress results of the thread.

The G105 drill pipe (material is 26CrMo) is taken as the research object in this paper. The material's performance parameters and fatigue curves are obtained by universal tensile test and multiracial fatigue test. A hexahedral mesh generation method for drill pipe body is proposed, and the joint thread node coordinates, node number automatic generation, and hexahedral mesh parametric modeling are realized by MATLAB software. Combined with elastic-plastic finite element technology, the distribution law of mechanical properties of drill pipe materials under different working conditions is analyzed and its life prediction is carried out. It provides a theoretical basis for the design and safety evaluation of drill pipe joints.

2. Mechanical Properties of Drill Pipe Materials and Tension-Torsion Fatigue Test

2.1. Experiments on Mechanical Properties of Drill Pipe Materials

The G105 drill pipe material 26CrMo was tested on a microcomputer-controlled electronic universal testing machine according to the international tensile test standard. The test temperature was 25 °C and the tensile rate was 0.2mm/min [20]. The test specimens and test equipment are shown in Figure 1.

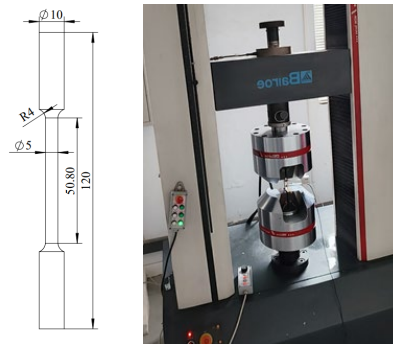


Figure 1: Experimental specimen size and experimental equipment diagram.

Table 1: Mechanical performance parameters of drill pipe materials

Mechanical Parameter	Value
Young's Modulus, E (MPa)	208000
Poisson's ratio, ν	0.28
Yield strength, σ_0 (MPa)	816
Tensile strength σ_b	896

Figure 2 shows the engineering stress-strain curve of the material of the drill pipe. Considering the geometry of the material, the processing precision, and the randomness of the experimental process, the average value of the experimental results of the six groups of specimens is taken as the mechanical property data of the material, and the tensile mechanical property parameters of the drill pipe joint material are shown in Table 1.

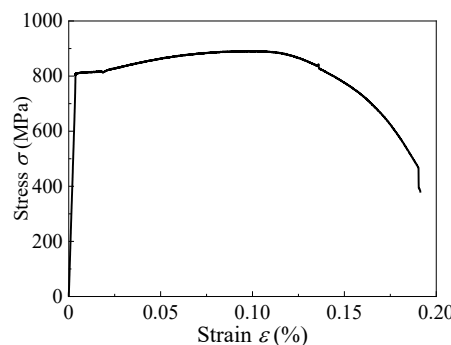


Figure 2: Engineering stress-strain curve of pipe body material.

2.2. Drill Pipe Material Tension-Torsion Fatigue Test

The tensile and torsional fatigue test of drill pipe material was carried out on a 250kN tensile and torsional fatigue test system. The loaded tensile stress ratio is -1, the loaded shear stress ratio is -1, the loading frequency is 3 Hz, the loading waveform is a triangular wave, and the test environment temperature is 34°C. The results of the tensile and torsion-al fatigue tests are shown in Table 2.

Table 2: Tension-torsion fatigue test results

No.	P_{\max}/kN	S_{σ}/MPa	$M_{\max}/\text{N}\cdot\text{m}$	τ_{σ}/MPa	N_f/Cycles
G1	11.44	444.5	33.47	311.15	1319
G2	10.29	400.05	30.12	280.04	2792
G3	9.72	377.8	28.45	264.48	17821
G4	9.15	355.6	26.78	248.92	51297
G5	8.58	333.4	25.10	233.36	125232
G6	8.01	311.15	23.43	217.81	251941
G7	6.86	266.7	20.08	186.69	1×10^6

3. Three-dimensional Parametric Modeling of Drill Pipe

3.1. Drill pipe body and joint transition section profiles and expressions

Figure 3 displays the outer contour of the transition section in the drill pipe. Where AB segment is the length of the transition section of the drill pipe, D is the outer diameter of the joint, d is the outer diameter of the pipe body, and R_k is the distance from a point on the transition section to the central axis.

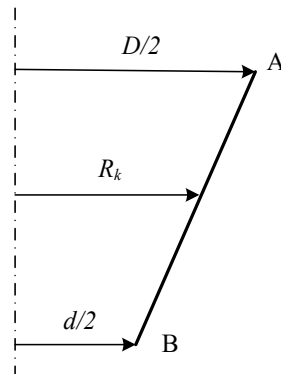


Figure 3: Outline of the transition section of the drill pipe.

Assuming that the transition section of the drill pipe is divided into c equal parts along the axial direction, the expression for the outer contour of the transition section of the drill pipe R_k ($k=1, 2, \dots, c+1$) can be expressed as follows.

$$R_k = \frac{D}{2} - \frac{k-1}{c} \left(\frac{D}{2} - \frac{d}{2} \right) \quad (1)$$

Similarly, the expression r_k can be obtained for the inner profile of the transition section of the drill pipe.

3.2. Construction of Parametric Model of Drill Pipe Transition Section.

Assuming that the inner diameter of the cross-section of the drill pipe transition section is r , a circle is established with the inner diameter r as the radius, and the outer diameter of the cross-section of the drill pipe transition section and the circle forms a ring. To partition the finite element mesh, the ring is subdivided into μ equal segments along the circumferential direction and v equal segments along the radial direction. As shown in Figure 4.

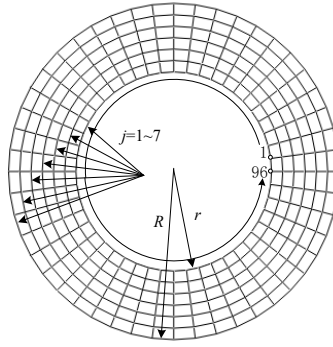


Figure 4: Diagram of the mesh division of the cross-section of the drill pipe (where $\mu = 96$ and $v = 7$).

Assuming $i=1, 2, \dots, \mu$, the angle between the nodes distributed along the circumference and the starting node is:

$$\theta = \frac{2\pi(i-1)}{\mu} \quad (2)$$

Assuming $j = 1, 2, \dots, v+1$, the distance from any node within the cross-section to the center axis of the drill pipe can be expressed as:

$$r_j = \frac{R-r}{v} \times (j-1) + r \quad (3)$$

Assuming that the length of the transition section of the drill pipe is l , the coordinates of the n th node can be expressed as:

$$\begin{bmatrix} x \\ y \\ z \end{bmatrix} = r_j \times \begin{bmatrix} \cos \theta \\ \sin \theta \\ 0 \end{bmatrix} + \begin{bmatrix} 0 \\ 0 \\ l(k-1)/c \end{bmatrix} \quad (4)$$

The node number can be expressed as:

$$N = \mu \times (v+1) \times (k-1) + \mu \times (j-1) + i \quad (5)$$

According to Equation (4) and Equation (5), the node number and node coordinates required for the finite element mesh of the drill pipe can be obtained. Then, the adjacent 8 nodes are connected to obtain the hexahedral element.

Suppose that the node label of the m th unit is n , and the node numbering order is shown in Figure 5. The 8 node numbers of the unit are shown in Table 3. The hexahedral mesh of the drill pipe transition section is shown in Figure 6.

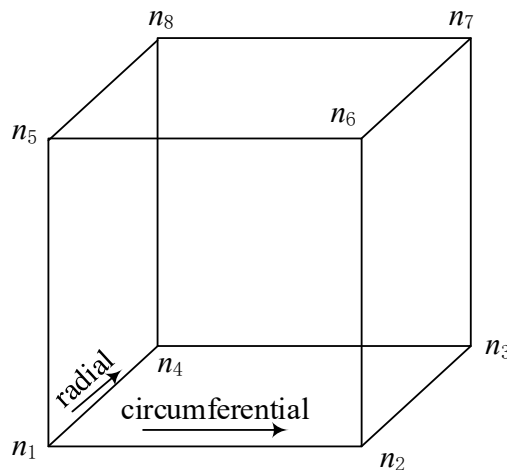


Figure 5: Schematic diagram of node number of unit m .

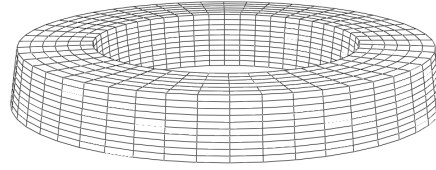


Figure 6: Hexahedral meshing of drill pipe transition section.

Table 3: Node number of element m

i Node number	1, 2, ..., $\mu-1$	μ
n_1	n	n
n_2	$n+\mu$	$n+\mu$
n_3	$n+\mu+1$	$n+1$
n_4	$n+1$	$n-\mu+1$
n_5	$n+\mu \times (v+1)$	$n+\mu \times (v+1)$
n_6	$n+\mu \times (v+2)$	$n+\mu \times (v+2)$
n_7	$n+\mu \times (v+2)+1$	$n+\mu \times (v+2)+1$
n_8	$n+\mu \times (v+1)+1$	$n+\mu \times (v+1)+1$

Similarly, all node numbers, node coordinates, and node number information of each unit of the drill pipe body can be obtained by referring to the 3D finite element modeling method of the transition section. With the help of MATLAB software, the parametric modeling of the drill pipe body and the transition section is realized, and the inp file is generated. The inp file is loaded into the ABAQUS program, and the 3D finite element model of the drill pipe body is finally obtained by Boolean operation and compression of coincidence nodes.

3.3. Establishment of Finite Element Model of Drill Pipe

Taking the directional drilling pipe of a company as the research object, the constitutive model of the material is based on the mechanical performance test results, and the structural parameters are shown in Table 4. The 3D finite element mesh model of the drill pipe transition section and the pipe section can be obtained by using the parametric modeling process. According to the geometric data of the inner diameter and outer diameter of the Pin and the length of the transition section, according to the parametric modeling process of Section 3.2, the MATLAB program is written to obtain the three-dimensional grid node information and unit information, and the inp file is automatically generated. The inp file is loaded into the ABAQUS program for the merge operation, and the three-dimensional finite element grid model of the drill pipe is obtained, as shown in Figure 7. In order to improve the calculation accuracy and efficiency, fine meshing is used in the transition section, and sparse meshing is used in other parts, and the number of drill pipe mesh units is 169920.

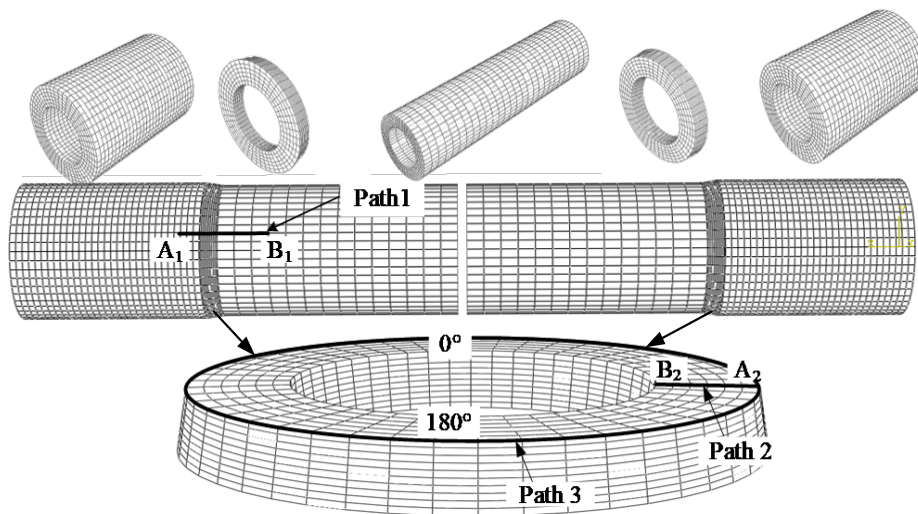


Figure 7: Parameterized grid model of drill pipe.

Table 4: Thread parameters of drill pipe.

Parameter	Value
Outer diameter of the joint (mm)	76
Joint wall thickness (mm)	10
Joint length (mm)	110
Outer diameter of pipe body (mm)	73
Wall Thickness of Pipe body (mm)	5.51
Pipe body length (mm)	3000
Length of transition section (mm)	10

3.4. Calculation and Application of Drill Pipe Loads

In the context of drilling activities, it is common for the drill pipe to undergo bending, resulting in the generation of bending moments due to the applied bending force. In engineering practice, the degree of bending of the borehole is characterized by the borehole curvature, which can be expressed as the curvature of the drill pipe according to the planar elastic beam theory [19]:

$$\frac{1}{\rho} = \frac{M}{EI} \quad (6)$$

Where ρ is the radius of curvature of the drill pipe, M is the bending moment borne by the drill pipe, E is the modulus of elasticity of the drill pipe material, and I is the moment of inertia of the drill pipe. When the length of the drill pipe is 3 m, the relationship between the borehole curvature β and the radius of curvature is:

$$\rho = \frac{3}{\sin \beta} \quad (7)$$

$$M = \frac{EI}{3} \sin \beta \quad (8)$$

If the outer diameter D_m and inner diameter d_m of the drill pipe are known, I can be expressed as:

$$I = \frac{\pi D_m^4}{64} \left(1 - \left(\frac{d_m}{D_m} \right)^4 \right) \quad (9)$$

According to the structure and material parameters of the drill pipe, the joint bending load at different borehole curvatures can be obtained as shown in Table 5.

Table 5: The relationship between hole curvature and bending load.

Curvature (°/3 m)	1	2	3	4	5
Bending moment (kN·m)	1.398	2.795	4.191	5.586	6.979

4. Results and discussion

4.1. Mechanical Characterization of Drill Pipe Materials under Torsion

The elastic-plastic finite element method was used to simulate the mechanical properties of the drill pipe under torque, and Fig. 8 shows the stress state of the drill pipe material when the torque is 4000 N·m. From the figure, it can be seen that the stress distribution on the equal-wall section of the drill pipe is very uniform, the stress increases along the radial direction, and the maximum value of the stress appears on the outer surface of the drill pipe body, with the maximum value of 194.1 MPa. The stress on the transition section decreases in the axial direction with the increase of the wall thickness.

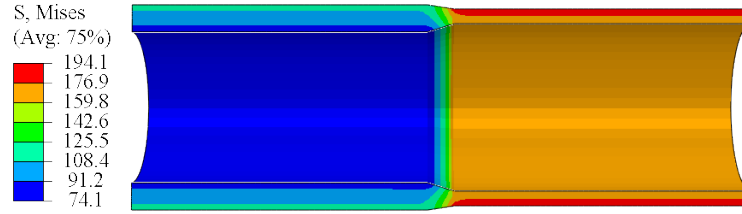


Figure 8: Stress distribution cloud of drill pipe under torsional loads

Torque loads of $T_1 = 4000 \text{ N}\cdot\text{m}$, $T_2 = 5000 \text{ N}\cdot\text{m}$, $T_3 = 6000 \text{ N}\cdot\text{m}$, $T_4 = 7000 \text{ N}\cdot\text{m}$, and $T_5 = 8000 \text{ N}\cdot\text{m}$ were applied to the drill pipe, and Figure 9(a) and (b) show the stress distribution characteristics of the drill pipe under the effect of different torques from axial (Path1) and radial (Path2) directions, respectively. It can be seen that the stress distribution along the axial direction of the drill pipe is related to the wall thickness and torsional load, the smaller the wall thickness, the higher the stress on the surface of the drill pipe, and the higher the torsional load, the higher the stress on the surface of the drill pipe. There is a sudden change of stress in the cross-section of the transition section in contact with the pipe body, and the stress generated here is the largest, which should be taken into account in the design process of the pipe body.

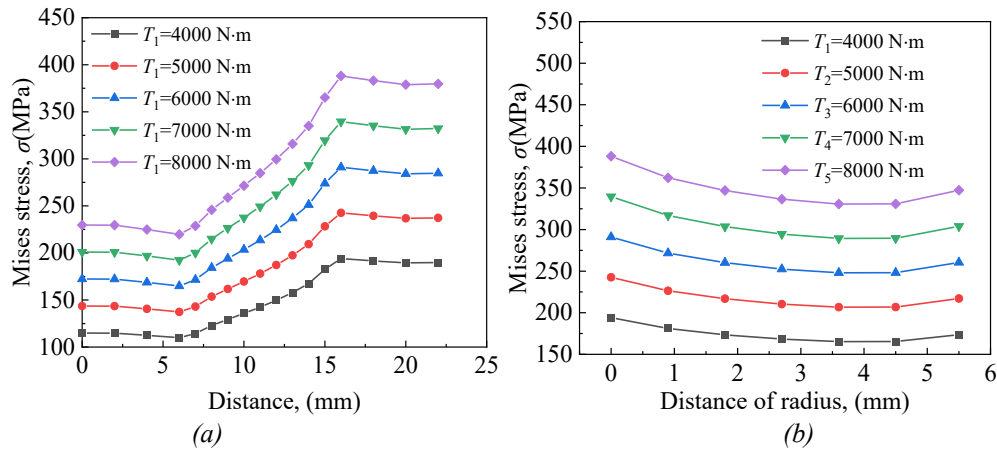


Figure 9: Stress distribution of drill pipe under different torque: (a) Distribution along path1 (b) Distribution along path2

4.2. Mechanical Characterization of Drill Pipe under Compound Load of Compression and Torsion

The drill pipe was subjected to compression-torsion composite loads to replicate the stress conditions. These loads included compression forces of 100 kN, 200 kN, 210 kN, 250 kN, and 300 kN, with a torque of 4000 N·m. When the compression load is 100 kN, the working stress distribution of the drill pipe is shown in Figure 10. It can be seen that the stress distribution characteristics of the drill pipe under compression-torsion composite loading are similar to those of the drill pipe when only the upper buckling torque is applied: the stresses are distributed more uniformly in the equal-wall section and increase along the radial direction, and the stress distribution along the axial direction in the transition section decreases with the increase of the wall thickness. However, under the compression-torsion composite load, the maximum stress of the drill pipe appeared on the inner surface of the drill pipe body with a maximum value of 217.4 MPa.

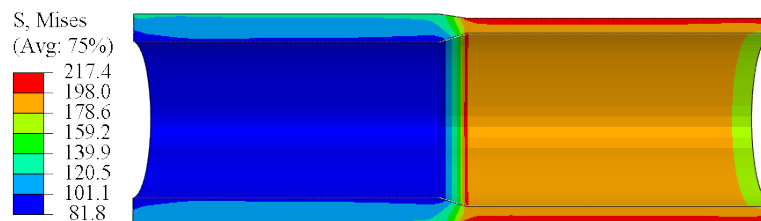


Figure 10: Stress distribution of drill pipe body under compressive-torsional composite loads

Figures 11(a) and (b) show the stress distribution characteristics along the axial (Path1) and radial

(Path2) directions of the drill pipe under the same torque with different compressive loads applied, respectively. The stress distribution of the drill pipe is influenced by both the compression load and the wall thickness. Notably, the highest stress is always seen at the minimal wall thickness during the transition section. With the increase of compression load, the stress distribution along the radial direction of the drill pipe shows that the state of the two sides is big, the middle is small, and the inner surface stress is gradually higher than the outer surface stress. Therefore, in order to enhance the longevity of the pipe body, it is important to strengthen its surface.

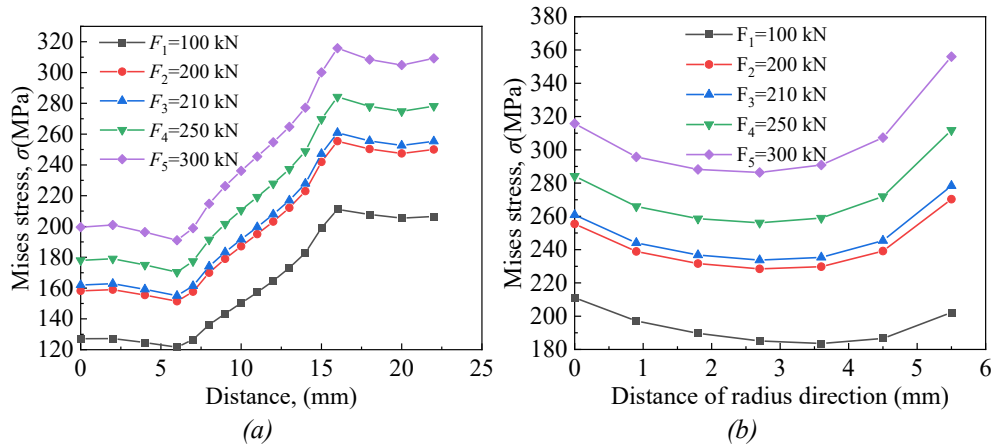


Figure 11: Stress distribution in drill pipe under compressive-torsional composite loads: (a) Distribution along path1 (b) Distribution along path2

4.3. Mechanical Characterization of Drill Pipe under Compression-Torsion-Bending Composite Loading

The working stress distribution characteristics of the G105 drill pipe are investigated under torque $T=4000$ N·m, axial pressure $F=100$ kN, and borehole curvature is taken as $0^\circ/3\text{m}$, $1^\circ/3\text{m}$, $2^\circ/3\text{m}$, $3^\circ/3\text{m}$, $4^\circ/3\text{m}$, and $5^\circ/3\text{m}$, respectively. Figure 12 illustrates the stress distribution of the drill pipe material when subjected to a borehole curvature of $1^\circ/3$ m. It can be seen that the stresses of the drill pipe under the composite load of compression, torsion, and bending show asymmetric distribution. Due to the bending moment, the bent drill pipe shows a state of tension on one side and compression on the other side, and the maximum stress value of 240 MPa appears on the compression side.

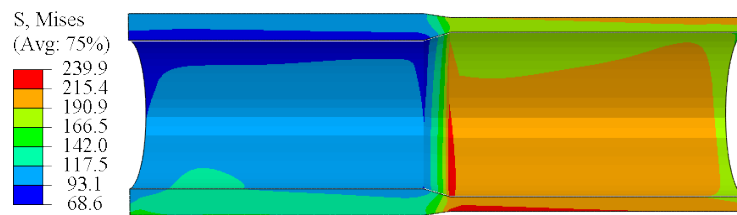


Figure 12: Stress distribution of drill pipe under compression-torsion-bending composite loads

Figures 13(a) and (b) show the stress distribution characteristics of the drill pipe along the axial (Path1) and circumferential (Path3) directions under the same torque and axial pressure, respectively, for different borehole curvatures. Figure 13(a) shows that under compression-torsion-bending composite loading also exhibits that the smaller the wall thickness, the higher the stress on the surface of the drill pipe. With the increase of borehole curvature, the gradient of stress growth along the radial direction of the drill pipe is increasing, so it can be seen that compared with the compression and torsion load, the bending moment load has the greatest influence on the stress distribution of the drill pipe. According to Figure 13(b), the stress distribution along the circumferential direction of the drill pipe exhibits symmetry when the borehole curvature is $0^\circ/3$ m. The stresses in the drill pipe are distributed symmetrically in the circumferential direction. As the bending moment load increases, the drill pipe's circumferential stress distribution becomes increasingly asymmetric, with the compression edge experiencing much greater stress.

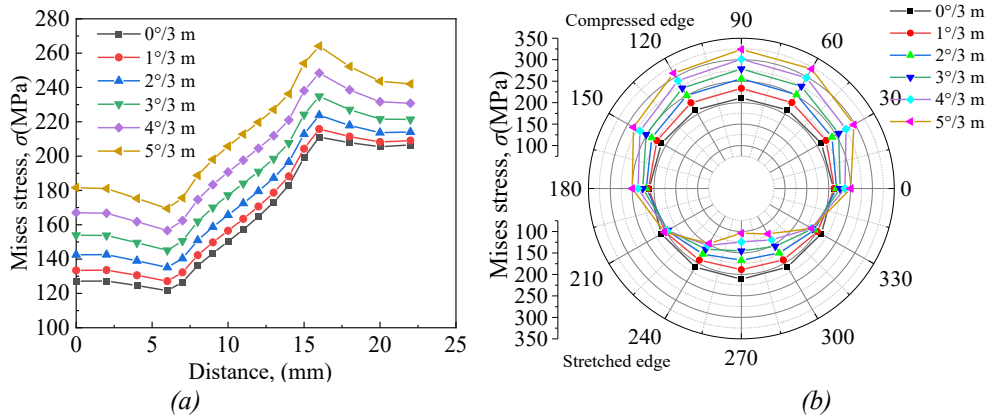


Figure 13: Stress distribution in drill pipe under compression-torsion-bending composite loads: (a) Distribution along path1 (b) Distribution along path3

4.4. Effect of Different Wall Thicknesses on The Mechanical Properties of Drill Pipe Materials.

The mechanical properties of the drill pipe material are closely related to the wall thickness. In order to realize the lightweight design of the drill pipe, under the conditions of torque $T = 6000 \text{ N}\cdot\text{m}$, axial pressure $F = 210 \text{ kN}$, and borehole curvature of $3^\circ/3\text{m}$, different drill pipe thicknesses $D_1 = 3.01$, $D_2 = 3.51$, $D_3 = 4.01$, $D_4 = 4.51$, $D_5 = 5.01$, $D_6 = 5.51$ are taken respectively. The analysis of the mechanical properties of the drill pipe material is depicted in Figure 14. The relationship between the wall thickness of the drill pipe and the stresses can be observed, indicating that as the wall thickness increases, the stresses decrease. To provide an adequate safety margin for the drill pipe, it is advisable to maximize the wall thickness of the drill pipe to a value more than 5 mm.

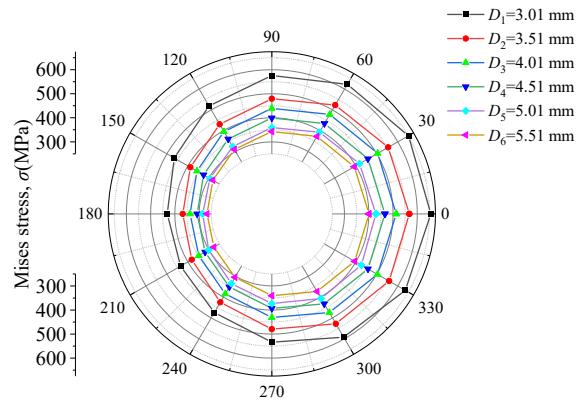


Figure 14: Stress distribution along Path3 for drill pipe with different wall thicknesses

4.5. Fatigue Life Prediction of Drill Pipe Materials.

According to the actual operation data of a company's drill pipe, the range of drilling pressure is set to $100 \text{ kN} \sim 300 \text{ kN}$, the range of torsional load is set to $4000 \text{ kN} \sim 8000 \text{ kN}$, and the range of borehole curvature is set to $1^\circ/3\text{m} \sim 3^\circ/3\text{m}$. Based on the stress of the drill pipe, the S-N curve of the 26CrMo material is defined, and the load time history is input to obtain the fatigue life distribution characteristics of the G105 drill pipe. As shown in Figure 15. It can be seen that the minimum fatigue life of the drill pipe occurs at the intersection of the transition section and the pipe body, and the minimum value of fatigue life is 2.1×10^6 cycles. Therefore, in order to improve the life of the drill pipe, the surface of the drill pipe here needs to be strengthened.

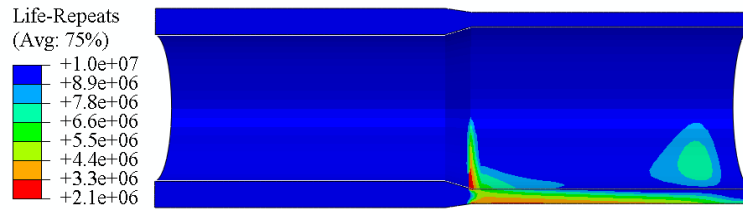


Figure 15: Fatigue life nephogram of drill pipe

The longevity of drill pipe is intricately linked to the thickness of its pipe body. When the thickness of the drill pipe is $D1=3.01$, $D2=3.51$, $D3=4.01$, $D4=4.51$, $D5=5.01$, $D6=5.51$, the relationship between the fatigue life of the drill pipe and the wall thickness is shown in Figure 16. It can be seen that the fatigue life of the drill pipe is positively correlated with the wall thickness: the service life of the drill pipe increases proportionally with the increased wall thickness of the pipe body.

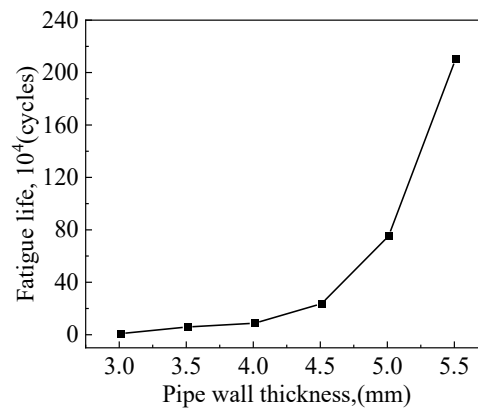


Figure 16: Relationship between fatigue life and wall thickness of drill pipe

5. Conclusions

1) A novel parametric modeling approach is introduced in this study, which takes into account the transition section of the drill pipe body. This technique is based on the design principles of rotation, lifting, and connecting nodes, and it utilizes the geometric expression of the cross-section profile perpendicular to the drill pipe axis.

2) The stress distribution on the G105 steel drill pipe body is related to the wall thickness under the combined loads of torque, tension torsion and tension-bending-torsion. The smaller the wall thickness is, the greater the stress on the surface of the drill pipe is. The increase of the torque will increase the stress on the outer surface of the pipe, and the increase of the compression load will increase the surface stress at the junction of the transition section and the pipe body.

3) The fatigue life of the drill pipe is positively correlated with the wall thickness: the greater the wall thickness of the pipe body, the longer the life of the drill pipe. The point of minimal multiaxial fatigue life for drill pipe is often found at the junction of the transition section and the pipe body. To enhance the fatigue life of the drill pipe, it is advisable to focus on optimizing the structure of this particular area or consider using surface strengthening treatments.

Acknowledgements

This work is supported by the Engineering Research Center of Expressway Construction & Maintenance Equipment and Technology of MOE Foundation, Chang'an University (300102253512).

References

[1] Shi, Z.J.; Yao, K.; Yao, N.P.; Li, Q.X.; Tian, H.L.; Dong, Z.; Wang, Q.F.; Yin, X.S.; Liu, F. 40 years of development and prospect on underground coal mine tunnel drilling technology and equipment in

China. Coal sci. technol. 2020, 48(04): 1-34.

[2] Zamani, S.M.; Hassanzadeh-Tabrizi, S.A.; Sharifi, H. Failure analysis of drill pipe: A review. *Eng. Fail. Anal.* 2016, 59: 605-623.

[3] Komissarov, A.A.; Ozherelkov, D.Y.; Sazonov, Y.B.; Ten, D.V.; Tokar, A.A. Causes of High-Strength Drill Pipes Failure. *Russian Metallurgy (Metally)*, 2021, 2021(4): 470-474.

[4] Lu, S.; Feng, Y.; Luo, F.; Qin, C.; Wang, X. Failure analysis of IEU drill pipe wash out. *Int. J. Fatigue* 2005, 27(10-12): 1360-1365.

[5] Liu, Y.; Lian, Z.; Lin, T.; Shen, Y.; Zhang, Q. A study on axial cracking failure of drill pipe body. *Eng. Fail. Anal.* 2016, 59: 434-443.

[6] Luo, S.J.; Wen, N.H.; Han, L.H.; Corrosion Fatigue Behavior of S135 Drill Pipe Steel in H2S Environment. *Mater. Mech. Eng.* 2017, 41(06): 44-48.

[7] Yu, Z.; Zeng, D.; Hu, S.; Zhou, X.; Lu, W.; Luo, J.; Meng, K. The failure patterns and analysis process of drill pipes in oil and gas well: A case study of fracture S135 drill pipe. *Eng. Fail. Anal.* 2022, 138: 106171.

[8] Han, Y.; Zhao, X.; Bai, Z.; Yin C. Failure analysis on fracture of a S135 drill pipe. *Procedia Mater. Sci.* 2014, 3: 447-453.

[9] Liu, Y.; Lian, Z.; Lin, T.; Li, F.; Chen, C. Fracture failure analysis on a drill pipe in directional drilling[M]//*Pipelines 2013: Pipelines and Trenchless Construction and Renewals—A Global Perspective*. 2013: 1543-1549.

[10] Ryu, Y.; Matzen, V.C. The nonlinear behavior of threaded piping connections: Application using a modified Ramberg-Osgood model. *Ocean Eng.* 2016, 127: 1-6.

[11] Chen, S.J.; Gao, L.X.; Zhang, Y. Loading Analysis on Threaded Connections with Local Tooth Shape Errors. *J. South China Univ. Techno.: Nat. Sci. Ed.* 2010, 36(6): 843-850.

[12] Tikhonov, V.S.; Baldenko, F.D.; Bukashkina, O.S.; Liapidevskii, V.Y. Effect of hydrodynamics on axial and torsional oscillations of a drillstring with using a positive displacement motor. *J. Pet. Sci. Eng.* 2019, 183: 106423.

[13] Yu, S.; Yuan, P.; Deng, K.; Liu, W.; Lin, Y.; Zhuang, J. Experimental and numerical study on the longitudinal-crack failure of double-shoulder tool joint. *Eng. Fail. Anal.* 2018, 91: 1-11.

[14] Luo, S.; Wu, S. Effect of stress distribution on the tool joint failure of internal and external upset drill pipes. *Mater. Des.* 2013, 52: 308-314.

[15] Di, Q.; Song, H.; Chen, F.; Zhang, H.; Wang, W.; Li, N. The effect of bending moment direction on tool joints: Working load limits under complex loads. *J. Nat. Gas Sci. Eng.* 2016, 35: 532-540.

[16] Fang, P.L.; Yong, G.L.; Xin, H.W.; Cai, H.L. Failure analysis of 127mm IEU G105 drill pipe wash out. *Eng. Fail. Anal.* 2011, 18(7): 1867-1872.

[17] Guo, W.H.; Wu, B.C. Fatigue Analysis of Drill Pipe Joint under Extreme Conditions. *Machinery*, 2020, 58(03): 41-45.

[18] Zhang, Z.; Zhu, X.H. Multiaxial fatigue life of drill pipe joint. *Acta Petrol. Sin.* 2019, 40(7): 839-845.

[19] Zhu, X.H.; Dong, L.L.; Tong, H. Mechanical behaviors of short-round thread of the API casing under combined load of stretching and bending moment. *Acta Petrol. Sin.* 2013, 34(01): 157-163.

[20] ISO 6892-1; Metallic materials- Tensile testing-Part 1: Method of test at room temperature. International Organization for Standardization: Geneva, Switzerland, 2019.